Macrocyclic Ligand Ring Size Effects. Part 2.[1] Synthetic, Structural and Electrochemical Studies of the Interaction of Ni^{II} with 14-Membered Tetraaza Macrocycles containing Fused Dibenzo Substituents†

Kenneth R. Adam,[a] Michael Antolovich,[a] Larry G. Brigden,[a] Anthony J. Leong,[a] Leonard F. Lindoy,*[,a] Philip J. Baillie,[b] Daljit K. Uppal,[b] Mary McPartlin,*[,b] Bhavini Shah,[b] Davide Proserpio,[c] Luigi Fabbrizzi*[,c] and Peter A. Tasker*[,d]

[a] *Department of Chemistry and Biochemistry, James Cook University, Queensland 4811, Australia*

[b] *Department of Applied Chemistry and Life Sciences, The Polytechnic of North London, London N7 8DB, UK*

[c] *Instituto di Chimica Generale ed Inorganica, Universita di Pavia, 27100 Pavia, Italy*

[d] *Imperial Chemical Industries, Colour and Fine Chemicals Business, Blackley, Manchester M9 3DA, UK*

A comparative study of the high- and low-spin complexes of Ni^{II} with two tetraaza dibenzo-substituted macrocycles incorporating 14-membered inner rings has been carried out. The results obtained are also compared with those for the analogous nickel(II) derivatives of 1,4,8,11-tetraazacyclotetradecane. Four X-ray structures of nickel complexes as well as the structure of one free ligand have been determined. These structures taken together with previous X-ray structural data and selected molecular mechanics calculations have enabled a detailed assessment of the effects of spin state and ligand substituent on the hole size and ring conformations adopted by individual complexes. A comparative electrochemical investigation of individual high- and low-spin complexes in the series has been performed.

The chemistry of Ni^{II} with tetraaza macrocycles has been extensively studied.[2] For example, complexes of the 14-membered saturated macrocycle cyclam (1,4,8,11-tetraaza-cyclotetradecane) have been the subject of numerous investigations as have the related alkyl-substituted derivatives of the Curtis type. A number of dibenzo-substituted ring systems of this general class displaying various degrees of ring unsaturation and substitution have been investigated by us[1,3,4] and others.[5–7] As an extension of these earlier studies, we now report an investigation of the interaction of Ni^{II} with the dibenzo-macrocycle L^1. The nickel complexes of L^1 are compared with those of the related dibenzo derivative L^2 as well as with the corresponding complexes of the fully saturated analogue L^3.

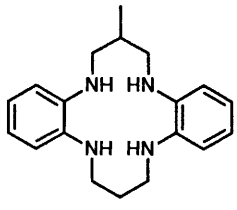

L^1

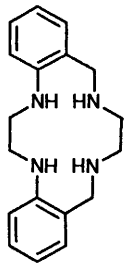

L^2

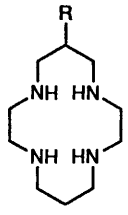

L^3 R = H
L^4 R = $C_{16}H_{33}$

Experimental

Physical measurements were performed as described previously.[4,8,9] Attempts to measure stability constants for the nickel complexes potentiometrically in 95% methanol (I = 0.1 mol dm^{-3}, NEt_4ClO_4) as described elsewhere[10] were unsuccessful because of low affinities, precipitation, and/or metal-catalysed ligand decomposition during the course of the titrations (as manifested by a marked darkening of the solution in the titration cell). Similar metal-catalysed oxidation of other anilino ligand systems has been reported previously.[11]

Molecular Mechanics Calculations.—These were based on Allinger's MM2 force field[12] and were performed using a suite of computer programs written at James Cook University. The minimisation of molecular geometry involved a quasi-Newton minimisation algorithm and Broyden–Fletcher–Goldfarb–Shanno (BFGS) update method with analytical first derivatives.

Electrochemical Studies.—The $E_{\frac{1}{2}}$ values for the $Ni^{III}LX_3$–$Ni^{II}LX_2$ (L = L^2) redox change were determined through voltammetric studies using a conventional three-electrode cell in which the working electrode was a platinum microsphere, the counter electrode was platinum foil, and the reference electrode was a silver wire. Deaerated solutions of the tetraalkyl-

† *Supplementary data available:* see Instructions for Authors, *J. Chem. Soc., Dalton Trans.*, 1991, Issue 1, pp. xviii–xxii.

ammonium carrier electrolytes were used as 0.1 mol dm^{-3} concentration containing the $NiLX_2$ complexes and ferrocene (internal standard to calibrate the pseudo-reference silver electrode) at 10^{-3} mol dm^{-3}. The electrochemical apparatus has been described previously.[13] EPR spectra of the chloronickel(III) complexes were determined in frozen acetonitrile solutions containing NEt_4Cl (0.1 mol dm^{-3}) following oxidation with nitrosonium tetrafluoroborate.

Synthetic Studies.—The syntheses and characterisation of ligands L^1,[1] L^2,[1] and L^4 (ref. 14) have been described previously.

(5,6,7,8,15,16,17,18-*Octahydro*-7-*methyl*-9H,14H-*dibenzo*-[b,i][1,4,8,11]*tetraazacyclotetradecine*)*nickel*(II) *tetrafluoroborate*, $[NiL^1][BF_4]_2$. To a hot solution of L^1 (ref. 4) (0.0126 g) in methanol (20 cm^3) under a nitrogen atmosphere was added nickel(II) tetrafluoroborate (0.0195 g) in hot methanol (20 cm^3). The resulting green solution was then evaporated slowly under nitrogen whereupon orange crystals of $[NiL^1][BF_4]_2$ were deposited. Yield: 0.0125 g (57%) (Found: C, 41.9; H, 4.7. $C_{19}H_{26}B_2F_8N_4Ni$ requires C, 42.0; H, 4.8%).

Diisothiocyanato(5,6,7,8,15,16,17,18-*octahydro*-7-*methyl*-9H,14H-*dibenzo*[b,i][1,4,8,11]*tetraazacyclotetradecine*)-*nickel*(II), $[NiL^1(NCS)_2]$. Nickel(II) tetrafluoroborate (0.1686 g) in hot methanol (20 cm^3) was added to L^1 (ref. 4) (0.1001 g) in methanol (10 cm^3) under nitrogen. Ammonium thiocyanate (0.0504 g) in methanol (5 cm^3) was added to the resulting green solution to yield a blue solution which was evaporated to a low volume under a nitrogen atmosphere. Pink needles of product were deposited. These were filtered off and washed with methanol. Yield: 0.0796 g (51%) (Found: C, 51.5; H, 5.4; N, 17.0. $C_{21}H_{26}N_6NiS_2$ requires C, 52.0; H, 5.4; N, 17.3%).

(5,6,7,8,9,10,15,16,17,18-*Decahydrodibenzo*[e,m][1,4,8,11]-*tetraazacyclotetradecine*)*nickel*(II) *tetrafluoroborate*, $[NiL^2][BF_4]_2$. A solution of the ligand (0.020 g) in chloroform (3 cm^3) was added to a solution of nickel(II) tetrafluoroborate (0.010 g) in methanol (3 cm^3). The solution was allowed to stand at room temperature and orange-red crystals appeared within 24 h. This product was filtered off, washed with cold methanol (2 cm^3) then dried under vacuum. Yield: 0.013 g (39%) (Found: C, 40.6; H, 4.5; N, 10.2. $C_{18}H_{24}B_2F_8N_4Ni$ requires C, 40.8; H, 4.6; N, 10.6%). Infrared (FTIR), ν_{max}/cm^{-1}: 3214, 3174, 2952, 2882, 1610, 1497, 1448, 1224, 1187, 1084, 1038, 1006 and 772. Electronic spectrum (dichloromethane), λ_{max}/nm ($\varepsilon/dm^3\ mol^{-1}\ cm^{-1}$): 457 (80).

(1,4,8,11-Tetraazacyclotetradecane)nickel(II)iodide,$[NiL^3]I_2$, was prepared from the correspondi..g diperchlorate salt[15] by the literature method.[16] Suitable crystals for the X-ray study were obtained by slow recrystallisation of the brown complex from a methanol–diethyl ether mixture.

X-Ray Structure Determinations. Crystal data. L^1, $C_{19}H_{26}N_4$, $M = 310.45$, monoclinic, space group $P2_1/c$, $a = 12.843(2)$, $b = 5.449(1)$, $c = 23.839(4)$ Å, $\alpha = 90$, $\beta = 101.52(2)$, $\gamma = 90°$, $U = 1634.51$ Å^3, $Z = 4$, $D_c = 1.261$ g cm^{-3}, $F(000) = 672$, μ(Mo-Kα) = 0.42 cm^{-1}.

$[NiL^1][BF_4]_2$, $C_{19}H_{26}B_2F_8N_4Ni$, $M = 542.76$, triclinic, space group $P\bar{1}$, $a = 9.200(2)$, $b = 8.549(2)$, $c = 7.994(2)$ Å, $\alpha = 109.10(2)$, $\beta = 112.91(2)$, $\gamma = 74.17(2)°$, $U = 538.22$ Å^3, $Z = 1$, $D_c = 1.67$ g cm^{-3}, $F(000) = 540$, μ(Mo-Kα) = 9.20 cm^{-1}.

$[NiL^1(NCS)_2]$, $C_{21}H_{26}N_6NiS_2$, $M = 485.31$, monoclinic, space group $P2_1/n$, $a = 13.210(2)$, $b = 15.926(3)$, $c = 11.184(2)$ Å, $\alpha = 90$, $\beta = 103.05(2)$, $\gamma = 90°$, $U = 2292.15$ Å^3, $Z = 4$, $D_c = 1.41$ g cm^{-3}, $F(000) = 1016$, μ(Mo-Kα) = 9.85 cm^{-1}.

$[NiL^2][BF_4]_2$, $C_{18}H_{24}B_2F_8N_4Ni$, $M = 528.74$, monoclinic, space group $C2/c$, $a = 13.392(3)$, $b = 10.247(2)$, $c = 15.725(3)$ Å, $\alpha = 90$, $\beta = 101.08(3)$, $\gamma = 90°$, $U = 2117.68$ Å^3, $Z = 8$, $D_c = 1.66$ g cm^{-3}, $F(000) = 2096$, μ(Mo-Kα) = 9.34 cm^{-1}.

$[NiL^3]I_2$, $C_{10}H_{24}I_2N_4Ni$, $M = 512.85$, monoclinic, space group $P2_1/c$, $a = 7.551(2)$, $b = 12.900(3)$, $c = 8.883(2)$ Å, $\alpha = 90$, $\beta = 111.88(2)$, $\gamma = 90°$, $U = 802.95$ Å^3, $Z = 2$, $D_c = 2.14$ g cm^{-3}, $F(000) = 984$, μ(Mo-Kα) = 47.48 cm^{-1}.

Data were collected in the θ range 3–25° for all five structures and were processed using methods described previously.[17] No absorption corrections were applied. Equivalent reflections were averaged to give the following unique data with $I > 3\sigma(I)$: $[NiL^1][BF_4]_2$, 1108; L^1, 2870; $[NiL^1(NCS)_2]$, 1250; $[NiL^2][BF_4]_2$, 1376; $[NiL^3]I_2$, 1118.

The structure of the free ligand L^1 was solved using the centrosymmetric EES routine of the SHELX[18] program. The first calculated E map defined the locations of the 23 non-hydrogen atoms. All but two hydrogen atoms were located from a Fourier difference map. The latter, H(3a2) and H(7a), were included in calculated positions (C–H 1.08 Å) during refinement. Positional parameters for the 'found' hydrogen atoms were not refined and these atoms were assigned a common thermal parameter of 0.08 Å^2. All non-hydrogen atoms were assigned anisotropic thermal parameters in full-matrix refinement which converged at R and R' values of 0.1093 and 0.1051, respectively. During the final stages of refinement a Fourier difference map indicated some uncertainty concerning the position of the anilino hydrogen atom H(2aN). When this atom was removed from the Fourier synthesis three sites of electron density were detected near N(2a). The position eventually selected for H(2aN) (Table 1) in the final cycles of refinement was that which was associated with the mininum energy in a molecular mechanics calculation.

For $[NiL^1][BF_4]_2$ the space group was initially assumed to be $P\bar{1}$ which requires the nickel atom to be located at a centre of symmetry. Fourier synthesis revealed the sites of all the remaining non-hydrogen atoms with half occupancy for the methyl substituent C(3a). Refinement in the centrosymmetric space group $P\bar{1}$ yielded normal thermal parameters for all atoms and Fourier difference maps revealed electron-density maxima which could only be ascribed to hydrogen atoms. Consequently no attempt was made to refine the structure in the $P1$ space group. Four hydrogen atoms were not located in the Fourier difference maps. These, H(1a2), H(4a2), H(9a) and H(2b1) (the last at half occupancy), were included in calculated positions (C–H 1.08 Å) during refinement. Hydrogen atoms were assigned a common thermal parameter of 0.05 Å^2 and all non-hydrogen atoms were refined anisotropically. For $[NiL^1(NCS)_2]$ the position of the nickel atom was located from a Patterson synthesis and all non-hydrogen atoms and the anilino-hydrogen atoms were found in subsequent Fourier difference syntheses. Hydrogen atoms attached to carbon were all included in calculated positions. Disorder of the methyl substituents was detected in Fourier difference maps. Refinement of population parameters for carbon atoms attached to C(2a) and C(2b) in both equatorial and axial positions indicated predominantly equatorial substitution. Consequently in the final stages of refinement carbon atoms C(3ae) and C(3be) and attached hydrogen atoms were assigned half occupancy in these sites. There was some evidence for disorder of the carbon atoms C(1a), C(2a) and C(4a) in one of the propane bridges, but additional sites for these atoms could not be resolved from electron-density maps. Anisotropic thermal parameters were assigned to these atoms and to all heteroatoms. For $[NiL^2][BF_4]_2$ a Patterson synthesis defined the position of the nickel atom and resolved the potential ambiguity between $C2/c$ and Cc space groups. All the remaining non-hydrogen atoms were readily identified in Fourier difference syntheses. Hydrogen atoms were included in calculated positions. Nickel, nitrogen and fluorine atoms were assigned anisotropic thermal parameters in the final cycles of refinement. The symmetry of the space group and size of the unit cell for $[NiL^3]I_2$ required that the $[Ni(cyclam)]^{2+}$ be located on a centre of inversion and a Patterson synthesis located the iodine atom in the asymmetric unit. Using this assignment of the positions of the nickel and iodine atoms allowed all the remaining atoms, with the exception of one of the hydrogen atoms attached to C(6), to be located from Fourier difference syntheses.

Final values of R and R' were 0.0732 and 0.0723 for $[NiL^1][BF_4]_2$, 0.0849 and 0.0812 for $[NiL^1(NCS)_2]$, 0.0648 and 0.0704 for $[NiL^2][BF_4]_2$ and 0.0636 and 0.0626 for $[NiL^3]I_2$, respectively. Weighting schemes were as previously reported.[17] The final atomic coordinates are given in Table 1, selected bond lengths in Table 2, and selected torsion angles in Table 3 while details of the structures are shown in Fig. 1. The X-ray structure determination of $[NiL^2(NCS)_2]$ has been reported elsewhere.[4]

Additional material for all structures available from the Cambridge Crystallographic Data Centre comprises H-atom coordinates, thermal parameters, and remaining bond lengths and angles.

Results and Discussion

Metal Complex Synthesis.—Reaction of nickel(II) tetrafluoroborate with L^1 in methanol yielded the low-spin orange complex $[NiL^1][BF_4]_2$. When a similar reaction was carried out in the presence of ammonium thiocyanate the high-spin (pink) species $[NiL^1(NCS)_2]$ was obtained. A similar procedure to that just mentioned was used to prepare $[NiL^2][BF_4]_2$. The infrared spectrum of each product showed the expected bands for the co-ordinated macrocycle as well as for the respective associated anions. The NH stretching modes were observed at approximately 3200 and at 3214 and 3174 cm^{-1} for the low-spin complexes $[NiL^1][BF_4]_2$ and $[NiL^2][BF_4]_2$ respectively, while bands attributable to the tetrafluoroborate group occurred in the range 1040–1150 cm^{-1}. In the case of $[NiL^1(NCS)_2]$ the NH stretching mode was present at 3240 cm^{-1} while the thiocyanate stretch occurred at 2085 cm^{-1}. The latter falls in the range expected for a terminal N-bonded thiocyanate group.[19] For $[NiL^2(NCS)_2]$ the NH stretches were observed at 3272 and 3241 cm^{-1} while the thiocyanate stretch was present at 2072 cm^{-1}.

X-Ray Diffraction Studies.—The solid-state structures of the free ligand L^1 and the corresponding low- and high-spin nickel complexes, $[NiL^1][BF_4]_2$ and $[NiL^1(NCS)_2]$, have been determined in the present study [Fig. 1(*a*)–(*c*)]. Structures have also been obtained for the low-spin complexes of L^2 and L^3, $[NiL^2][BF_4]_2$ and $[NiL^3]I_2$ [Fig. 1(*d*) and (*e*)]. Comparison with previously determined structures of a low-spin complex of L^3,[20] high-spin complexes of L^2 (ref. 1) and L^3 (ref. 21) and of the free ligand L^2 (ref. 1) allows the effect of variation of metal radius on ligand conformations to be assessed. It also enables an assessment of the introduction of additional rigidity (in the form of fused benzene rings) as well as the introduction of weaker anilino donors on the co-ordination geometry to be made.

The low-spin complex $[NiL^1][BF_4]_2$ has a planar co-ordination geometry. The tetrafluoroborate anions are not co-ordinated to the nickel atom, the closest contacts being made by hydrogen bonding to the anilino nitrogen atoms: N(2a)–H ··· F(1) 1.89 Å and N(1a)–H ··· F(2) 2.06 Å [the latter involving the F(2) related by $x, -y, z$ to that in Table 1]. In contrast, the high-spin complex $[NiL^1(NCS)_2]$ has a *trans*-pseudo-octahedral geometry with the thiocyanate groups co-ordinated to the nickel in axial sites through their nitrogen atoms.

The compound $[NiL^1][BF_4]_2$ is located on a crystallographic inversion centre which relates atoms in parts a and b of co-ordinated L^1; the presence of the centre is in accordance with disorder of the methyl substituent (see below). To allow comparison of the respective N_4-donor cavities in Table 4, the centroid of the N_4-donor set of the free ligand L^1 was substituted for the position of the nickel atom. Otherwise, in the case of L^1 the atom labelling is identical to that used for $[NiL^1(NCS)_2]$. The N_4-donor set is planar in $[NiL^1][BF_4]_2$ as a consequence of the crystallographic inversion centre, and very close to planar in the other two structures L^1 and $[NiL^1(NCS)_2]$. The latter have slight 'tetrahedral' displacements of the donors of ± 0.04 and ± 0.01 Å, respectively, from the corresponding least-squares planes. The nickel atom deviation from the N_4 plane is 0.025 Å for $[NiL^1(NCS)_2]$. This deviation is associated with a slight distortion from the pseudo-octahedral geometry towards a square pyramid, giving significantly different nickel to thiocyanate bond lengths (see Table 2).

Both L^1 and its complexes have a pseudo-mirror plane perpendicular to the mean plane of the molecule and passing through the central atoms of the propane bridges. For all three structures the six-membered rings have chair conformations, consistent with the pseudo-mirror molecular symmetry. For $[NiL^1][BF_4]_2$ there is one chair above and the other below the N_4-donor plane giving an overall 'step' arrangement [see Fig. 1(*c*)]. This arrangement corresponds to the low-energy *trans*-III isomer often observed for complexes of cyclam.[1] For $[NiL^1(NCS)_2]$ the two chair chelate rings fall on the same side of the N_4 plane [Fig. 1(*b*)], corresponding to the *trans*-I form of cyclam complexes. In this arrangement the aniline hydrogen atoms are all displaced to the same side of the N_4 plane, whereas in the 'step' arrangement found for $[NiL^1][BF_4]_2$ two hydrogens are above and two hydrogens are below the N_4 plane.

For the free Ligand L^1 [Fig. 1(*a*)] there is some ambiguity associated with the location of the anilino hydrogen atom H(2aN) attached to N(2a). One of the electron-density maxima detected near N(2a) in the X-ray structure determination corresponds to a hydrogen site giving an arrangement similar to that in $[NiL^1(NCS)_2]$ [which has four hydrogen atoms equally displaced to the same side of the N_4 plane, see Fig. 1(*b*)]. However, an alternative position which involves a weak hydrogen-bonding interaction with the lone pair on N(1a) was found to be associated with a lower strain energy by molecular mechanics calculation and was used in the final stages of structure refinement.

For low-spin $[NiL^1][BF_4]_2$ [Fig. 1(*c*)] the N_4 plane and the benzene rings are almost coplanar. In contrast, for both the high-spin $[NiL^1(NCS)_2]$ complex and the free ligand L^1 there is considerable deviation from planarity and in each case the benzene rings are inclined at $33 \pm 2°$ to the same side of the respective N_4 planes, resulting in 'saddle-shaped' arrangements.

In the low-spin complex $[NiL^2][BF_4]_2$ [Fig. 1(*d*)] the displacement of the benzene rings to the opposite sides of the NiN_4 plane is typical of other complexes of 14-membered macrocycles which have this pattern of fusion of two *o*-benzo groups on to the inner great ring.[4] The resulting configurations of the nitrogen donors correspond to the *trans*-V conformation.[23] For the cyclam complex $[NiL^3]I_2$ [Fig. 1(*e*)] the classic *trans*-III arrangement is observed [Fig. (1*e*)] with the co-ordination geometry being very similar to that found in the corresponding monohydrate structure reported earlier.[20]

Torsion angles in the inner great rings of the macrocycle provide a useful way of examining how co-ordination of high- and low-spin nickel(II) ions influences ligand geometry. For the free ligand L^1 the most favourable delocalisation of lone pairs on the sp^2-hybridised anilino nitrogen atoms will occur when the C_{ar}–C_{ar}–N–CH_2 torsion angles are close to 180° (see bonds *c*, *e*, *j*, *l* in Table 3). When the low-spin Ni^{II} is co-ordinated to the macrocycle in $[NiL^1][BF_4]_2$ the metal lies in the plane of the *o*-phenylenediamine unit. This, coupled to the change to sp^3 hybridisation at the anilino nitrogen atoms, leads to C_{ar}–C_{ar}–N–CH_2 torsion angles close to 120° (bonds *c*, *e*, *j*, *l* in Table 3). For the high-spin complex there is a considerable expansion of the N_4-donor cavity to accommodate the larger metal ion (see later). This is associated with a 'flattening' of the molecule leading to an increase in the C_{ar}–C_{ar}–N–CH_2 angle to *ca.* 150° (see Table 3). The flattening is very marked in the diaminopropane chelate rings where torsion angles involving the methylene unit (bonds *a*, *g*, *h*, *n* in Table 3) increase from values less than 70° in $[NiL^1][BF_4]_2$ to *ca.* 80° in $[NiL^1(NCS)_2]$. Bonds related by the pseudo-mirror planes in L^1, $[NiL^1][BF_4]_2$, and $[NiL^1(NCS)_2]$ (*e.g.* *a* with *n*, *b* with *m*, *etc.*) have torsion angles with similar values but opposite handedness.

The torsion angle data in Table 3 suggest that, for the more flexible macrocycles L^2 and L^3, conformational changes are

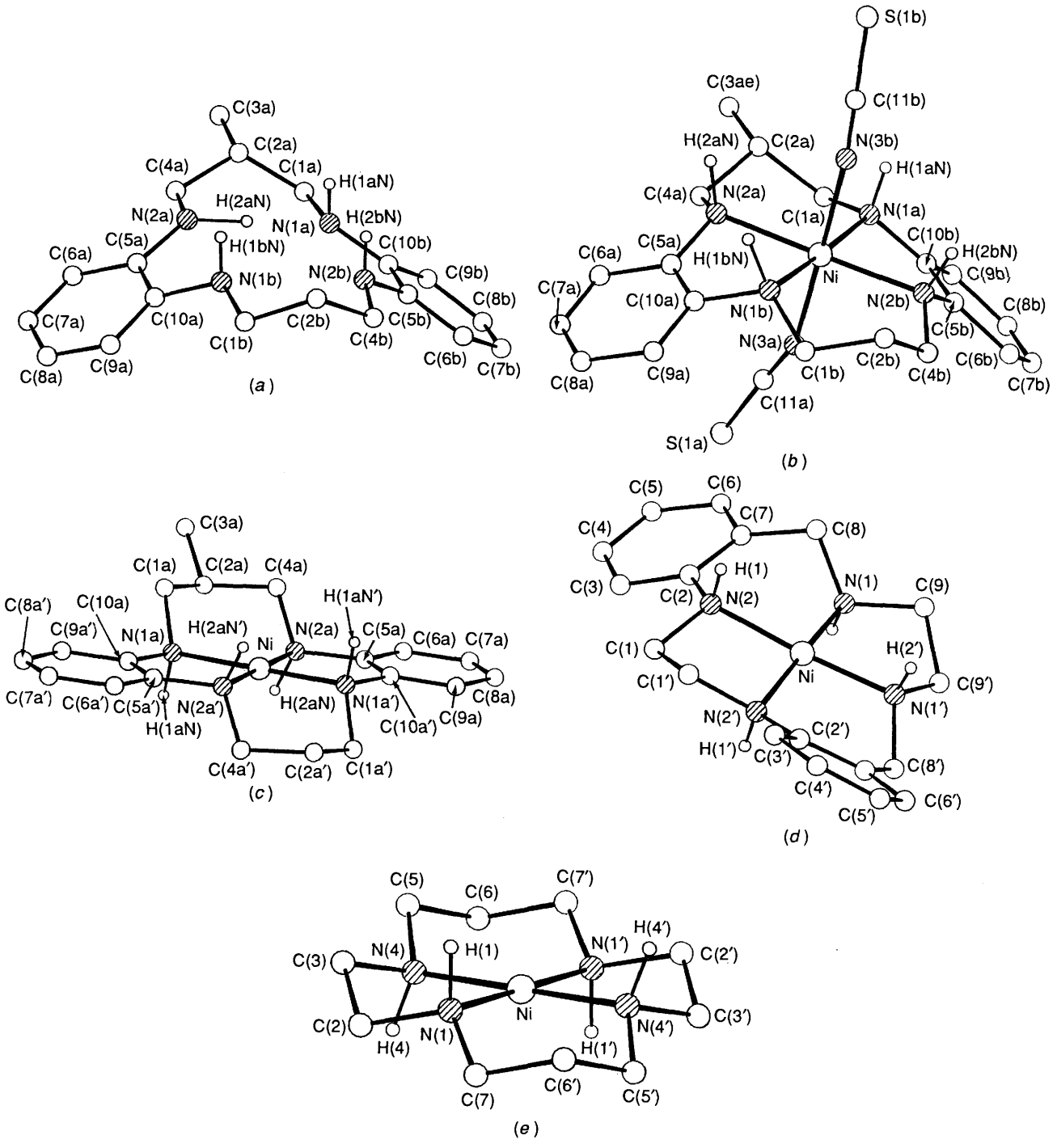

Fig. 1 View of (*a*) the free ligand L^1 and the nickel complexes (*b*) $[NiL^1(NCS)_2]$, (*c*) $[NiL^1][BF_4]_2$, (*d*) $[NiL^2][BF_4]_2$ and (*e*) $[NiL^3]I_3$, showing the differences in the configurations of the two- and three-carbon links between the nitrogen atoms

distributed more equally around the ring in 'opening out' or 'closing up' the N_4-donor sets to accommodate the (larger) high-spin Ni^{II} or (smaller) low-spin Ni^{II}, respectively.

A feature of interest in the complexes of L^1 is the positioning of the methyl substituent on the respective propane bridges. Axial or equatorial substitution is possible. There is also a possibility that a form of disorder will occur in the solid state in which the methyl-substituted propane bridge is found to be randomly distributed on either side of the sites occupied by the macrocyclic complex; it may only be the presence of the methyl group which breaks a perfect inversion centre or mirror-plane relationship between the two 'aliphatic' halves of the molecules. For L^1 no disorder was observed in the structure and the methyl group is solely equatorial. In the case of the low-spin complex $[NiL^1][BF_4]_2$ successful refinement of the structure in a centrosymmetric space group requires that the cationic complex lies on a crystallographic inversion centre coincident with the nickel atom; electron density corresponding to 'half' an equatorial methyl group was found adjacent to each propane bridge. In high-spin $[NiL^1(NCS)_2]$ there is no crystallographic imposition of disorder but nevertheless the methyl substituent was found to be evenly distributed on the two propane bridges (predominantly in equatorial sites, see Experimental section).

Inclinations of the thiocyanato groups to the co-ordination planes defined by the macrocycles vary significantly for the different high-spin complexes; Ni–N–CS angles are 156 and 163° in $[NiL^1(NCS)_2]$, 156° in $[NiL^2(NCS)_2]$[1] and 156–168° in the four crystallographically independent molecules of

Table 1 Fractional atomic coordinates with estimated standard deviations in parentheses

Atom	*x*	*y*	*z*	Atom	*x*	*y*	*z*
(*a*) $[NiL^1][BF_4]_2$							
Ni	0.000 00	0.000 00	0.000 00	C(7a)	0.415 5(12)	−0.071 6(15)	0.629 9(13)
N(1a)	−0.142 5(9)	0.201 5(9)	−0.059 7(10)	C(8a)	0.440 2(12)	−0.234 4(14)	0.527 6(16)
N(2a)	0.088 5(8)	0.115 2(8)	0.258 6(9)	C(9a)	0.355 8(12)	−0.280 7(12)	0.340 8(14)
C(1a)	−0.245 4(11)	0.277 0(11)	0.061 7(13)	C(10a)	0.237 2(10)	−0.163 0(11)	0.255 9(12)
C(2a)	−0.144 2(12)	0.341 4(12)	0.261 9(14)	F(1)	0.198 4(7)	0.356 5(7)	0.163 8(8)
C(3a)[a]	−0.241 5(24)	0.448 7(25)	0.371 7(27)	F(2)	0.103 4(8)	1.318 1(10)	−0.147 5(9)
C(4a)	−0.032 5(11)	0.199 9(11)	0.352 2(12)	F(3)	0.255 8(8)	0.111 2(7)	−0.021 4(9)
C(5a)	0.211 8(10)	0.000 6(11)	0.359 7(11)	F(4)	0.362 9(8)	0.322 5(8)	0.003 0(9)
C(6a)	0.298 0(12)	0.046 0(12)	0.544 5(13)	B	0.234 9(14)	0.280 9(14)	0.000 0(16)
(*b*) Ligand L^1							
N(1a)	0.816 1(7)	0.048 3(21)	0.113 5(4)	C(9a)	0.466 4(10)	−0.431 8(27)	0.183 4(6)
N(2a)	0.601 5(7)	0.078 6(23)	0.129 0(4)	C(10a)	0.542 1(10)	−0.257 9(29)	0.177 2(6)
N(1b)	0.648 4(7)	−0.254 3(23)	0.209 6(4)	C(1b)	0.679 8(10)	−0.457 6(28)	0.251 0(6)
N(2b)	0.865 9(7)	−0.270 4(21)	0.199 2(4)	C(2b)	0.795 2(9)	−0.422 9(27)	0.279 1(5)
C(1a)	0.780 5(9)	0.224 1(28)	0.066 9(5)	C(4b)	0.875 8(9)	−0.463 2(25)	0.241 0(5)
C(2a)	0.688 0(9)	0.373 1(26)	0.076 4(5)	C(5b)	0.925 8(9)	−0.286 1(27)	0.155 9(5)
C(3a)	0.662 9(10)	0.569 9(29)	0.030 0(6)	C(6b)	1.003 1(9)	−0.454 7(27)	0.154 3(5)
C(4a)	0.586 1(9)	0.243 8(28)	0.079 6(6)	C(7b)	1.055 0(10)	−0.456 6(31)	0.108 6(7)
C(5a)	0.518 1(10)	−0.076 3(29)	0.134 4(6)	C(8b)	1.027 9(11)	−0.300 0(33)	0.063 5(6)
C(6a)	0.415 8(10)	−0.069 1(29)	0.102 0(6)	C(9b)	0.952 0(10)	−0.128 0(26)	0.065 7(6)
C(7a)	0.340 3(9)	−0.236 3(34)	0.110 3(6)	C(10b)	0.898 1(9)	−0.118 0(26)	0.110 3(6)
C(8a)	0.365 8(11)	−0.418 7(30)	0.149 1(7)				
(*c*) $[NiL^1(NCS)_2]$							
Ni	0.213 5(2)	0.110 4(1)	0.348 2(2)	C(9a)	0.113 5(15)	0.328 7(12)	0.496 1(20)
S(1a)	−0.143 5(4)	0.150 0(5)	0.186 0(8)	C(10a)	0.162 4(13)	0.273 5(10)	0.425 2(18)
S(1b)	0.581 7(3)	0.110 7(3)	0.358 7(5)	C(11a)	−0.026 2(14)	0.128 2(11)	0.255 1(17)
N(1a)	0.214 3(12)	0.023 4(9)	0.206 7(18)	C(1b)	0.181 0(14)	0.166 5(11)	0.593 1(18)
N(2a)	0.211 7(12)	0.222 2(8)	0.243 4(15)	C(2b)	0.235 3(16)	0.083 0(12)	0.644 1(19)
N(3a)	0.055 1(11)	0.110 3(9)	0.308 0(14)	C(4b)	0.179 4(15)	0.005 5(12)	0.558 6(20)
N(1b)	0.218 4(10)	0.198 6(8)	0.486 5(15)	C(5b)	0.164 3(12)	−0.063 9(10)	0.357 3(16)
N(2b)	0.217 9(10)	−0.002 1(7)	0.449 6(14)	C(6b)	0.115 2(13)	−0.135 1(10)	0.401 2(19)
N(3b)	0.378 0(10)	0.109 8(9)	0.384 6(15)	C(7b)	0.060 8(14)	−0.188 6(13)	0.307 1(20)
C(1a)	0.173 7(24)	0.052 5(14)	0.079 3(24)	C(8b)	0.058 1(15)	−0.176 7(13)	0.190 7(20)
C(2a)	0.229 1(24)	0.141 7(15)	0.057 5(21)	C(9b)	0.108 4(14)	−0.107 7(12)	0.148 6(20)
C(4a)	0.172 6(17)	0.214 6(15)	0.114 7(25)	C(10b)	0.164 5(13)	−0.051 0(11)	0.240 1(18)
C(5a)	0.159 3(14)	0.281 8(12)	0.308 4(20)	C(11b)	0.462 4(13)	0.110 0(11)	0.373 2(15)
C(6a)	0.099 2(15)	0.349 2(12)	0.237 3(21)	C(3ae)[a,b]	0.225 30	0.153 60	−0.071 60
C(7a)	0.052 7(15)	0.403 2(14)	0.308 5(21)	C(3be)[a,b]	0.209 60	0.064 30	0.772 60
C(8a)	0.055 3(15)	0.397 4(15)	0.424 6(21)				
(*d*) $[NiL^2][BF_4]_2$							
Ni	0.000 00	0.199 89(10)	0.250 00	C(3)	0.135 8(5)	−0.008 9(7)	0.079 1(4)
N(2)	0.010 3(4)	0.062 8(4)	0.166 2(3)	C(4)	0.185 8(5)	0.016 1(8)	0.009 6(5)
N(1)	0.023 5(4)	0.334 6(5)	0.172 5(3)	C(5)	0.169 0(6)	0.127 2(7)	−0.037 1(5)
F(1)	0.282 5(3)	0.998 8(4)	−0.195 5(3)	C(6)	0.104 2(5)	0.221 3(7)	−0.015 9(5)
F(2)	0.363 2(3)	0.838 7(5)	−0.112 9(3)	C(7)	0.053 6(4)	0.201 5(6)	0.052 9(4)
F(3)	0.317 5(5)	0.810 5(5)	−0.252 5(3)	C(8)	−0.011 0(4)	0.306 0(6)	0.078 7(4)
F(4)	0.198 9(3)	0.820 2(5)	−0.169 4(4)	C(9)	−0.016 2(4)	0.459 9(6)	0.201 8(4)
C(1)	0.033 4(4)	−0.061 3(6)	0.216 6(4)	B	0.289 8(6)	0.866 0(8)	−0.183 2(5)
C(2)	0.069 2(4)	0.084 7(6)	0.098 5(4)				
(*e*) $[NiL^3]I_2$							
I	−0.240 08(11)	0.021 52(7)	0.242 70(10)	N(4)	0.248 6(13)	0.020 2(7)	0.171 4(12)
Ni	0.000 00	0.000 00	0.000 00	C(5)	0.290 5(17)	0.119 8(11)	0.267 1(14)
N(1)	0.026 8(13)	−0.143 1(7)	0.070 2(12)	C(6)	0.252 2(19)	0.213 1(10)	0.153 1(18)
C(2)	0.231 7(19)	−0.162 8(10)	0.177 0(16)	C(7)	0.044 8(19)	0.228 0(9)	0.050 8(17)
C(3)	0.297 7(18)	−0.069 7(11)	0.282 5(14)				

[a] Assigned a site occupation factor of 0.5. [b] Positional parameters not included in the final refinements (see text).

$[NiL^3(NCS)_2]$.[21] Such a difference, which is also observed in other diisothiocyanatonickel derivatives of macrocyclic ligand complexes,[19,24] may be a consequence of intermolecular interactions in the solid state. Thus, the two thiocyanato sulphur atoms are involved in weak hydrogen bonds to neighbouring anilino groups in $[NiL^1(NCS)_2]$ and the different inclinations of the two isothiocyanates appear related to the different intermolecular NCS • • • HN interactions present.

The bond lengths in the inner great rings of L^1–L^3 and their nickel complexes are given in Table 2. With the exception of bonds involving C(1a), C(2a) and C(4a) in $[NiL^1(NCS)_2]$ which show signs of disorder, bond lengths fall within the expected ranges. The marked lengthening of the benzene to nitrogen bonds (*c*, *e*, *l* and *j* in L^1 and *b* and *f* in L^2, see Table 2) on formation of nickel complexes is a consequence of the change in hybridisation of the nitrogen atoms and is consistent with the changes in torsion angles noted above.

The two crystallographically independent Ni–N(anilino) bonds in the low-spin $[NiL^1][BF_4]_2$ complex have similar lengths, as do the Ni–N(aliphatic) bonds in $[NiL^3]I_2$. In

Table 2 Bond lengths in the inner great rings and bonding cavities L^1 L^3 and their low- and high-spin nickel(II) complexes

Bond[a]	$[NiL^1][BF_4]_2$[b]	L^1	$[NiL^1(NCS)_2]$	Bond[a]	$[NiL^2][BF_4]_2$[d]	L^2	$[NiL^2(NCS)_2]$[d]
a C(2b)–C(4b)	1.53(1)	1.52(2)	1.63(3)	*a* C(7a)–C(2a)	1.391(9)	1.41(1)	1.407(4)
b C(4b)–N(2b)	1.47(1)	1.44(2)	1.43(3)	*b* C(2a)–N(2a)	1.459(9)	1.391(9)	1.450(4)
c N(2b)–C(5b)	1.45(1)	1.41(2)	1.49(2)	*c* N(2a)–C(1a)	1.499(7)	1.449(9)	1.481(4)
d C(5b)–C(10b)	1.38(1)	1.41(2)	1.33(3)	*d* C(1a)–C(1b)	1.51(1)	1.534(9)	1.533(8)
e C(10b)–N(1a)	1.44(1)	1.40(2)	1.44(3)	*e* C(1b)–N(2b)	*d*	1.47(1)	*d*
f N(1a)–C(1a)	1.49(1)	1.47(2)	1.48(3)	*f* N(2b)–C(2b)	*d*	1.407(9)	*d*
g C(1a)–C(2a)	1.51(1)	1.49(2)	1.64(4)	*g* C(2b)–C(7b)	*d*	1.41(1)	*d*
h C(2a)–C(4a)	*b*	1.50(2)	1.59(4)	*h* C(7b)–C(8b)	*d*	1.51(1)	*d*
i C(4a)–N(2a)	*b*	1.46(2)	1.42(3)	*i* C(8b)–N(1b)	*d*	1.480(9)	*d*
j N(2a)–C(5a)	*b*	1.39(2)	1.46(3)	*j* N(1b)–C(9b)	*d*	1.471(9)	*d*
k C(5a)–C(10a)	*b*	1.41(2)	1.31(3)	*k* C(9b)–C(9a)	1.49(1)	1.51(1)	1.526(7)
l C(10a)–N(1b)	*b*	1.43(2)	1.49(2)	*l* C(9a)–N(1a)	1.497(8)	1.46(1)	1.476(4)
m N(1b)–C(1b)	*b*	1.49(2)	1.48(3)	*m* N(1a)–C(8a)	1.487(8)	1.48(1)	1.485(4)
n C(1b)–C(2b)	*b*	1.51(2)	1.56(3)	*n* C(8a)–C(7a)	1.481(9)	1.51(1)	1.520(4)
Ni–N(2b)	1.920(6)	2.00(2)[c]	2.114(13)	Ni–N(2a)	1.949(5)	2.04(1)[c]	2.091(2)
Ni–N(1a)	1.931(7)	1.93(2)[c]	2.106(18)	Ni–N(2b)	*d*	1.98(1)[c]	*d*
Ni–N(2a)	*b*	1.96(2)[c]	2.129(14)	Ni–N(1b)	*d*	2.05(1)[c]	*d*
Ni–N(1b)	*b*	1.89(2)[c]	2.079(15)	Ni–N(1a)	1.908(5)	2.03(1)[c]	2.046(2)
Ni–NCS			2.040(14)	Ni–NCS			2.108(2)
Ni–NCS			2.119(13)				

	$[NiL^3]I_2$[b]	L^3[e]	$[NiL^3(NCS)_2]$[f]
a C(6′)–C(7′)	1.502(17)	1.541	1.519(7)
b C(7′)–N(1)	1.488(15)	1.460	1.474(4)
c N(1)–C(2)	1.505(15)	1.462	1.480(5)
d C(2)–C(3)	1.490(18)	1.539	1.510(12)
e C(3)–N(4)	1.478(16)	1.462	1.473(6)
f N(4)–C(5)	1.507(17)	1.460	1.478(5)
g C(5)–C(6)	1.529(19)	1.541	1.513(5)
Ni–N(1)	1.935(9)	2.054[c]	2.074(7)
Ni–N(4)	1.944(8)	2.054[c]	2.074(7)
Ni–NCS			2.121(9)

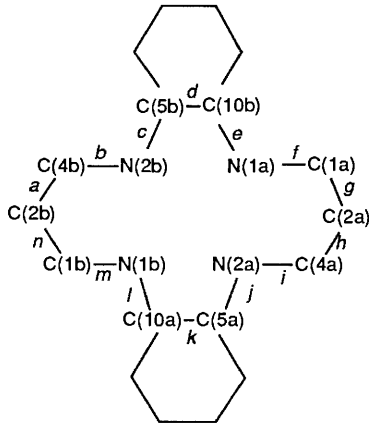

L^1

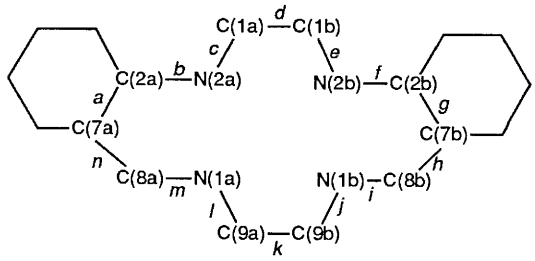

L^2

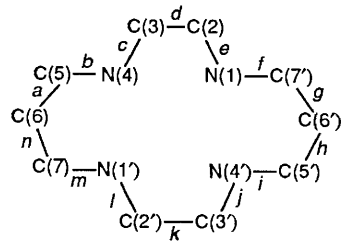

L^3

[a] Bonds in the inner great rings are labelled *a* to *n* as shown. [b] The molecule has an inversion centre coincident with the nickel atom, therefore *a* = *n*, *b* = *m*, *etc.* [c] Distance to centroid of donor atom set. [d] The molecule lies on a crystallographic C_2 axis passing through the nickel atom and the midpoints of the ethane bridges, therefore *a* = *g*, *b* = *f*, *etc.* [e] Values from molecular mechanics calculations (see text). [f] This structure has four crystallographically independent complexes, each of which resides at a centre of symmetry. Values quoted are means for the chemically equivalent bonds in each.

contrast, as expected, in $[NiL^2][BF_4]_2$ the Ni–N lengths differ significantly with much stronger bonds being formed by the more basic aliphatic nitrogen donors.

The correlation between axial and in-plane co-ordination bond lengths in high-spin diisothiocyanatonickel(II) complexes has been discussed previously by Ito *et al.*[21] A comparison of the complexes of the ligands L^1–L^3 shows a similar trend to that outlined by these authors (see Table 2). The stronger-field ligands L^2 and L^3 containing the more strongly basic (aliphatic) nitrogen donors give complexes in which bonds to the axial NCS groups are longer than the in-plane Ni–N bonds. The converse is true for the weaker-field (all anilino donor) ligand L^1, although the situation is complicated in this latter case by the non-equivalence of the Ni–NCS bond lengths (see above).

Hole Size Considerations.—The 'hole sizes' in the macrocyclic ligands L^1–L^3 and in their low- and high-spin nickel(II) complexes are given in Table 4; R_H values have been calculated from the X-ray structural data as the mean distance of the nitrogen-donor atoms from their centroids using procedures described previously.[22] The results suggest that 14-membered ring ligands of the cyclam type, which give an alternating sequence of 5,6,5,6-membered chelate rings, have 'natural' hole sizes which lie between those which are ideal for low- and high-spin nickel(II) ions. This is consistent with the observation that

Table 3 Torsion angles (°) in the inner great rings of the macrocycles

Bond[a]	$[NiL^1][BF_4]_2$[b]	L^1	$[NiL^1(NCS)_2]$	$[NiL^2][BF_4]_2$	L^2[b]	$[NiL^2(NCS)_2]$	$[NiL^3]I_2$	L^3[c]	$[NiL^3(NCS)_2]$[d]
a	66	69	81	7	2	5	68	66	70
b	170	−174	−173	−177	−175	−171	177	−178	−179
c	125	168	152	178	−170	173	174	176	170
d	1	1	−2	−56	−62	−59	−52	−61	−57
e	124	−178	−154	178	−174	173	174	176	170
f	171	176	176	−177	−166	−171	176	−178	−179
g	68	62	−80	7	0	5	67	66	70
h	−66	64	81	52	55	60	−68	−66	−70
i	−170	−173	−174	165	−179	170	−177	178	179
j	−125	170	156	173	168	168	−174	−176	−170
k	−1	1	−2	−55	−70	−61	52	61	57
l	−124	−174	−151	173	162	168	−174	−176	−170
m	−171	178	174	165	178	170	−176	178	179
n	−68	−69	−80	52	53	60	−67	−66	−70

[a] See footnotes to Table 2 for bond labels and symmetry equivalences. [b] For ease of comparison the signs of the torsion angles for this compound have been reversed from those on the asymmetric unit listed in Table 1. [c] Values from molecular mechanics (see text). [d] See footnote *f*, Table 2.

Table 4 Macrocyclic hole sizes (R_H) and bonding-cavity radii (R_A) for cyclam L^3 and the dibenzocyclam ligands L^1 and L^2 as well as for their respective low- and high-spin nickel complexes

	Low-spin complex $[NiL^1][BF_4]_2$	Free ligand L^1	High-spin complex $[NiL^1(NCS)_2]$
R_H[a]	1.93	1.95	2.11
R_A[a]	1.21		1.39
R_A/R_p[a]	1.01		1.00
	$[NiL^2][BF_4]_2$	L^2	$[NiL^2(NCS)_2]$
R_H	1.93	2.02[b]	2.07
R_A	1.21		1.35
R_A/R_p	1.01		0.97
	$[NiL^3]I_2$	L^3	$[NiL^3(NCS)_2]$
R_H	1.94	2.05[c]	2.07
R_A	1.22		1.35
R_A/R_p	1.02		0.97

[a] The values of R_H, R_A were calculated as described in ref. 22; R_p is the appropriate Pauling covalent radius for high- or low-spin nickel; R_A/R_p gives an indication of the match of the Ni^{II} to the macrocyclic cavity (R_A/R_p = 1 corresponds to an ideal match). [b] Value from ref. 4*b*. [c] Value from molecular mechanics calculations (see text).

these ligands can accommodate either type of ion, depending on whether co-ordinating or non-co-ordinating anions are present. In every case incorporation of the low-spin Ni^{II} appears to require a 'closing up' of the N_4-donor set (decrease in R_H) from that observed in the free ligand, while the incorporation of the high-spin ion requires an 'opening up' of the donor set (increase in R_H). While this generalisation is empirically sound, care is needed in making a detailed analysis of differences between hole sizes in the free ligands and their nickel complexes, since the conformations of the free ligands may differ significantly from the conformations which are suitable for effective co-ordination to a metal ion. Thus for ligand L^2 the 'natural' hole size is associated with the conformation based on intramolecular hydrogen bonding between the anilino protons and the benzylamino nitrogen atoms and has effectively sp^2 hybridisation of the anilino nitrogen atoms.[4] These features minimise strain in the free ligand but are eventually lost (see above) on metal complex formation. Similar changes in intramolecular hydrogen bonding and in donor-atom hybridisation are not a feature of complex formation by cyclam (L^3) which incorporates only aliphatic donors.

The 'goodness of fit' of the ligands for low- and high-spin Ni^{II} in their complexes can be compared using the 'bonding cavity' radii R_A (Table 4) in which an allowance has been made for the observed covalent radii of the nitrogen donors in nickel complexes.[22] Values are consistent with the proposal that these ligands would provide a 'best fit' for a metal ion with a covalent radius intermediate between that of low- and high-spin Ni^{II}.

Molecular Mechanics Studies.—The molecular mechanics calculations were based on Allinger's MM2 force field. Force-field parameters for those parts of the respective molecules involving the Ni^{II} were derived for each series of high- and low-spin complexes using a trial-and-error procedure based on X-ray data for a wide range of related (N_4-donor) macrocyclic complexes taken from the literature.[25] It is noted that the inclusion of an out-of-plane bending term for the nickel and donor set resulted in a slightly better fit for compounds of the present type. Starting from the X-ray coordinates, good agreement was obtained for $[NiL^1][BF_4]_2$, $[NiL^2][BF_4]_2$ and $[NiL^2(NCS)_2]$; however, for $[NiL^1(NCS)_2]$ the match was less than satisfactory. The mimimised structure of $[NiL^1(NCS)_2]$ had the two benzene rings approximately coplanar, while in the X-ray structure they form a V shape [see Fig. 1(*b*)]. The crystal-packing diagram for $[NiL^1(NCS)_2]$ indicates that the closest contacts between the benzene rings of different molecules are approximately 3.5 Å but would be much closer if the more planar geometry predicted by the molecular mechanics calculations was adopted (and related crystal packing maintained). Hence intermolecular interaction between aromatic rings in adjacent molecules appears likely to make a major contribution to the above observed difference between the X-ray and minimized structures. It is noted that no account of intermolecular contacts is allowed for in the present molecular mechanics treatment which hence generates 'gas phase' structures. The unsatisfactory fit for $[NiL^1(NCS)_2]$ is illustrated by the data for this complex in Table 5. For the high-spin complexes no attempt was made to model the thiocyanate ligands since their orientations are very susceptible to crystal-packing forces. For this reason their contributions to the root mean square calculations were not included.

In molecular mechanics studies of the present type it is also important to perform a number of parallel calculations starting from different sets of starting coordinates in order to confirm that a given calculated structure corresponds to the true minimum-energy geometry for the system. Hence, in the present study new starting coordinates were generated by manipulation of the original (X-ray) coordinates such that, for example, various stereoisomers corresponding to the five *trans* structures theoretically possible for $[Ni(cyclam)]^{2+}$ were generated.[23] Relative energies of these isomers are in Table 6.

In all cases but $[NiL^1][BF_4]_2$ the molecular mechanics calculations indicated that the isomers observed by X-ray diffraction are in each case predicted to be favourable arrangements, even though, for three systems, alternative

Table 5 Differences in parameters between X-ray and calculated structures of the nickel(II) complexes of L^1–L^3; root mean square (r.m.s.) values with maximum deviations

	$[NiL^1(NCS)_2]$[a]	$[NiL^1][BF_4]_2$	$[NiL^2(NCS)_2]$	$[NiL^2][BF_4]_2$	$[NiL^3]I_2$	$[NiL^3(NCS)_2]$
r.m.s. bond (Å)	(0.055)	0.026	0.011	0.022	0.017	0.019
Max. deviation	(0.099)	0.039[b]	0.025	0.042	0.029	0.040
r.m.s. angle (°)	(3.9)	1.3	1.2	1.9	1.8	1.3
Max. deviation	(8.1)	2.9	2.3	3.5	4.4	3.0
r.m.s. torsion angle (°)	(21.2)	4.3	2.1	2.4	2.8	1.4
Max. deviation	(69.5)	7.5[c]	4.1	5.2	5.3	2.8

[a] Structure minimised to a different configuration to that from the X-ray diffraction (see text). [b] Excluding disordered methyl group (maximum 0.1008 Å). [c] Excluding disordered methyl group (maximum 10.2°).

Table 6 Relative total steric energies[a] (kJ mol^{-1}) for the *trans* isomers of the high- and low-spin nickel(II) complexes of L^1 and L^2[b]

	trans I		*trans* II		*trans* III		*trans* IV		*trans* V	
Complex	Equatorial[c]	Axial	Equatorial	Axial	Equatorial	Axial	Equatorial	Axial	Equatorial	Axial
$[NiL^1(NCS)_2]$[d]	2.0	7.1	17.5	17.3	0.0	6.1	22.2	22.2	54.4	54.4
$[NiL^1][BF_4]_2$[e]	0.0	7.9	36.3	44.3	11.9	19.0	57.7	57.7	93.8	93.8

	trans I	*trans* II	*trans* III	*trans* IV	*trans* V
$[NiL^2(NCS)_2]$[f]	48.7	13.3	32.0	60.1	0.0
$[NiL^2][BF_4]_2$[f]	15.7	0.0	17.4	17.9	4.4

[a] Energies relative to the lowest-energy configuration set to zero. [b] It should be noted that, since the force field for the elements of the structures involving the respective central nickel atoms has not been calibrated in terms of energy, the relative energies quoted for each structure must be considered as approximate. [c] The terms equatorial and axial refer to the position of the methyl group on L^1. [d] Configuration observed in X-ray structure is *trans* I equatorial. [e] Configuration observed in X-ray structure is *trans* III equatorial. [f] Configuration observed in X-ray structure is *trans* V.

Table 7 The $E_{\frac{1}{2}}$ values (V) for the Ni^{II} to Ni^{III} conversion relative to the ferrocenium–ferrocene couple

Complex	Solvent	Electrolyte	$E_{\frac{1}{2}}$
$[NiL^3][ClO_4]_2$	CH_3CN	$[NBu_4][ClO_4]$	0.59[a]
$[NiL^2][ClO_4]_2$	CH_3CN	$[NBu_4][ClO_4]$	0.47[a]
$[NiL^2Cl_2]$	CH_3CN	$[NBu_4]Cl$	0.16[a]
$[NiL^4][ClO_4]_2$	CH_2Cl_2	$[NBu_4][ClO_4]$	0.92[b]
$[NiL^2][ClO_4]_2$	CH_2Cl_2	$[NBu_4][ClO_4]$	0.56[a]
$[NiL^4Cl_2]$	CH_2Cl_2	$[NBu_4]Cl$	0.18[b]
$[NiL^2Cl_2]$	CH_2Cl_2	$[NBu_4]Cl$	0.23[a]

[a] This work. [b] From ref. 14.

isomers were indicated to be of comparable stabilities (see below). However, for $[NiL^1][BF_4]_2$ the calculations indicated that the isomer corresponding to *trans* I was significantly lower in energy than that corresponding to the *trans* III; this is not the expected order, since the latter isomer is the one observed by X-ray diffraction. Nevertheless, the energy difference between the isomers remains relatively small at 12 kJ mol^{-1} (note that this value is only approximate as the parts of the force field involving the nickel have not been calibrated in terms of energy) and examination of the individual energy components reveals that the differences occur almost exclusively in the van der Waals interactions. It seems quite likely that crystal-packing energies could well dominate in such a situation but in the absence of additional information it appears inappropriate to speculate further on the reason(s) for the above observation. In the case of $[NiL^1(NCS)_2]$ the calculations indicated that the *trans* I isomer had a comparable energy to the *trans* III isomer observed in the X-ray structure.

It is noted that for both $[NiL^2(NCS)_2]$ and $[NiL^2][BF_4]_2$ molecular mechanics correctly predicts that the adoption of an uncommon *trans* V configuration for the respective co-ordinated macrocycles will be in each case favourable, although, for $[NiL^2][BF_4]_2$, the calculations indicate that an arrangement corresponding to *trans* II is also of similar energy to the *trans* V arrangement found experimentally. Similarly, in the case of the low-spin nickel complex of L^3, the *trans* I arrangement was calculated to be of similar energy to that of the observed *trans* III geometry.

Electrochemical Studies.—Aliphatic tetraazamacrocycles are known[1] to be effective in stabilising nickel in higher oxidation states. The very strong in-plane interactions exerted by tetraazamacrocycles raise the energy of the antibonding orbital (essentially metallic in character) from which the electron is extracted on oxidation. In this sense, the strongly co-ordinating 14-membered framework of cyclam is particularly efficient in promoting access to nickel(III) state.[26] The incorporation of fused benzene rings into tetraaza macrocycles will introduce weakly basic anilino nitrogen atoms and thus might be expected to provide a donor set which is less effective in stabilising the higher-oxidation-state ion. This in turn might be expected to result in higher (more positive) potentials for the Ni^{III}–Ni^{II} couple. In the present study, surprisingly, the opposite trend was observed in making comparisons between the complexes of cyclam L^3 and its dibenzo analogue L^2. Thus, when acetonitrile was used as the solvent, the oxidation of $[NiL^2][ClO_4]_2$ was found to occur at a slightly lower potential than that for $[NiL^3][ClO_4]_2$ (see Table 7). However, interpretation of the results obtained in this solvent tends to be complicated by two factors: (*i*) the divalent complexes may exist as low- and high-spin species, according to a ratio which varies with the type of macrocycle present; (*ii*) the anion (*e.g.* ClO_4^-) may compete with solvent molecules for axial co-ordination in the case of the low-spin trivalent complexes.

To reduce solvent effects electrochemical investigations on some of the nickel complexes were repeated in dichloromethane; the latter is a weakly polar, non-co-ordinating solvent. In order to obtain sufficient solubility in this solvent, a more lipophilic version of cyclam, namely *N*-cetylcyclam L^4, was used. In the latter studies it was observed that, in the case of the complexes containing perchlorate, the oxidation process Ni^{II} to Ni^{III} in the complex of the diaminodianilino macrocycle L^2 now takes place at a potential (0.56 V *vs.* ferrocenium–ferrocene) which is considerably less positive than measured for the complex of L^4 (0.92 V).

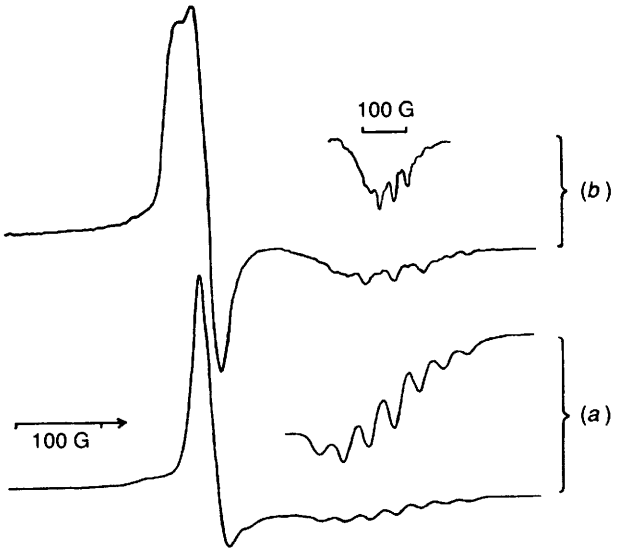

Fig. 2 The EPR spectra of frozen actonitrile solutions of the nickel(III) complexes derived from $[NiL^2Cl_2]$, (*a*) in the presence of added $[NBu_4]Cl$ ($g_\perp = 2.190$, $g_\parallel = 2.025$, $A_\parallel = 27.56$) consistent with the formulation $[NiL^2Cl_2]^+$ and (*b*) in the absence of added chloride ($g_\perp = 2.190$, $g_\parallel = 2.025$, $A_\parallel = 32.50$) consistent with replacement of axial Cl^- by CH_3CN; G = 10^{-4} T

The structure determinations discussed previously in this paper indicate that there is no significant difference in 'hole size' between cyclam and its dibenzo analogue L^2 which might otherwise account for an increased planar ligand field to stabilise Ni^{III} in $[NiL^2]^{3+}$. One possible explanation for the unexpectedly favourable conversion $Ni^{II} \longrightarrow Ni^{III}$ between the complexes of L^2 lies in conformational differences in the six-membered chelate rings relative to the situation for co-ordinated cyclam. Thus, there is significantly less puckering of these chelate rings in the complexes of L^2. As a consequence, the ClO_4^- or BF_4^- anions will be able to make a closer approach to the metal centre in the nickel(III) complexes of L^2 and hence provide more favourable (partial) neutralisation of the cationic charge present in the weakly polar medium, dichloromethane.

The situation is different for the chloro complexes; $[NiL^2Cl_2]$ is oxidized as a potential which is slightly more positive than that observed for $[NiL^4Cl_2]$ (0.23 *vs.* 0.18 V *vs.* ferrocenium–ferrocene). This may be ascribed to the fact that, in the $[Ni^{II}LCl_2]$ (high spin) to $[Ni^{III}LCl_2]Cl$ (low spin) conversion, octahedral stereochemistry is maintained and no substantial contraction of the axial bonds occurs. Thus, the oxidation process Ni^{II} to Ni^{III} in the *N*-cetylcyclam L^4 complex would not be expected to be associated with any significant increase in steric repulsions between the axially bound anions and the puckered rings of the ligand. In contrast, very marked axial contraction will occur on passing from the essentially planar low-spin complex $[Ni^{II}L][ClO_4]_2$ to the octahedral $[Ni^{III}L(ClO_4)_2]ClO_4$ (low spin) complex. Such a contraction will lead to a more significant destabilisation of the trivalent complex of the fully saturated macrocycle L^4 because the approach of the ClO_4^- ion will tend to be hampered by the puckered chelate rings.

The possibility that ligand-based oxidation could be responsible for the low oxidation potentials of the complexes of the dibenzo ligand L^2 can be discounted from EPR data. Namely, formulation of the oxidation products as nickel(III) complexes is supported by EPR measurements on frozen solutions. For these measurements the products were generated by oxidation of the corresponding nickel(II) species with nitrosonium tetrafluoroborate in acetonitrile. In the presence of excess of chloride ion the EPR spectrum (Fig. 2) shows $g_\parallel$ signals characteristic of *trans*-dichloronickel(III) complexes. In the absence of added chloride, oxidation of $[NiL^2Cl_2]$ results in a more complex EPR spectrum suggesting partial dissociation of chloro-ligands under these conditions to yield a mixture of $[NiL^2Cl(CH_3CN)]^{2+}$ and $[NiL^2(CH_3CN)_2]^{3+}$.

Acknowledgements

We thank the SERC, NATO and ICI plc as well as the Australian Research Council for financial support.

References

1 K. R. Adam, B. J. McCool, A. J. Leong, L. F. Lindoy, C. W. G. Ansell, P. J. Baillie, K. P. Dancey, L. A. Drummond, K. Henrich, M. McPartlin, D. K. Uppal and P. A. Tasker, *J. Chem. Soc., Dalton Trans.*, 1990, 3435 and refs. therein.
2 L. F. Lindoy, *The Chemistry of Macrocyclic Ligand Complexes*, Cambridge University Press, Cambridge, 1989.
3 M. Green and P. A. Tasker, *Inorg. Chim. Acta*, 1971, **5**, 65; C. W. G. Ansell, M. F. H. Y. J. Chung, M. McPartlin and P. A. Tasker, *J. Chem. Soc., Dalton Trans.*, 1982, 2113; C. W. G. Ansell, M. McPartlin, P. A. Tasker and A. Thambythurai, *Polyhedron*, 1983, **2**, 83.
4 (*a*) L. A. Drummond, K. Henrick, M. J. L. Kanagasundaram, L. F. Lindoy, M. McPartlin and P. A. Tasker, *Inorg. Chem.*, 1982, **21**, 3923; (*b*) K. Henrick, L. F. Lindoy, M. McPartlin, P. A. Tasker and M. P. Wood, *J. Am. Chem. Soc.*, 1984, **106**, 1641.
5 H. Hiller, P. Dimroth, H. Pfitzner, *Justus Liebigs Ann. Chem.*, 1968, **717**, 137; A. R. Cutler and D. Dolphin, *J. Coord. Chem.*, 1976, **6**, 59; M. C. Weiss, G. Gordon and V. L. Goedken, *Inorg. Chem.*, 1977, **16**, 305; M. Hunziker, B. Hilti and G. Rihs, *Helv. Chim. Acta*, 1981, **64**, 82; V. B. Rana, P. Singh, D. P. Singh and M. P. Teotia, *Polyhedron*, 1982, **1**, 377; R. Hanke and E. Breitmaier, *Chem. Ber.*, 1982, **115**, 1657; K. Sakata, S. Wada, N. Sato, M. Kurisu, M. Hashimoto and Y. Kato, *Inorg. Chim. Acta*, 1986, **119**, 111; K. Sakata and M. Hashimoto, *Inorg. Chim. Acta*, 1988, **146**, 145.
6 H. Elias, R. Grewe, D.-D. Klaehn and H. Paulus, *Z. Naturforsch., Teil B*, 1984, **39**, 903.
7 D.-D. Klaehn, H. Paulus, R. Grewe and H. Elias, *Inorg. Chem.*, 1984, **23**, 483.
8 K. R. Adam, A. J. Leong, K. F. Lindoy, H. C. Lip, B. W. Skelton and A. H. White, *J. Am. Chem. Soc.*, 1983, **105**, 4645.
9 K. R. Adam, K. P. Dancey, A. J. Leong, L. F. Lindoy, B. J. McCool, M. McPartlin and P. A. Tasker, *J. Am. Chem. Soc.*, 1988, **110**, 8471.
10 D. E. Fenton, B. P. Murphy, A. J. Leong, L. F. Lindoy, A. Bashall and M. McPartlin, *J. Chem. Soc., Dalton Trans.*, 1987, 2543.
11 E. B. Fleischer, A. E. Gebala and P. A. Tasker, *Inorg. Chim. Acta*, 1972, **6**, 72.
12 N. L. Allinger, *J. Am. Chem. Soc.*, 1977, **99**, 8127.
13 P. S. Pallavicini, A. Perotti, A. Poggi, B. Seghi and L. Fabbrizzi, *J. Am. Chem. Soc.*, 1987, **109**, 5139.
14 G. De Santis, M. Di Casa, M. Mariani, B. Seghi and L. Fabbrizzi, *J. Am. Chem. Soc.*, 1989, **111**, 2422.
15 E. K. Barefield, F. Wagner, A. W. Heringer and A. R. Dahl, *Inorg. Synth.*, 1975, **16**, 220.
16 E. Iwamoto, K. Imai and Y. Yamamoto, *Inorg. Chem.*, 1984, **23**, 986.
17 M. K. Cooper, P. A. Duckworth, K. Henrick and M. McPartlin, *J. Chem. Soc., Dalton Trans.*, 1981, 2357.
18 G. M. Sheldrick, SHELX crystal structure solving package, University of Cambridge, 1976.
19 G. A. van Albada, R. A. G. de Graaff, J. G. Haasnoot and J. Reedijk, *Inorg. Chem.*, 1984, **23**, 1404; K. R. Adam, A. J. Leong, L. F. Lindoy, B. J. McCool, A. Ekstrom, I. Liepa, P. A. Harding, K. Henrick, M. McPartlin and P. A. Tasker, *J. Chem. Soc., Dalton Trans.*, 1987, 2537.
20 L. Prasad and A. McAuley, *Acta Crystallogr., Sect. C*, 1983, **39**, 1175.
21 T. Ito, M. Kato and H. Ito, *Bull. Chem. Soc. Jpn.*, 1984, **57**, 2641.
22 K. Henrick, P. A. Tasker and L. F. Lindoy, *Prog. Inorg. Chem.*, 1985, **33**, 1.
23 B. Bosnich, C. K. Poon and M. L. Tobe, *Inorg. Chem.*, 1965, **4**, 1102.
24 G. M. Freeman, E. K. Barefield and D. G. van Derveer, *Inorg. Chem.*, 1984, **23**, 3092.
25 K. R. Adam, M. Antolovich, L. G. Brigden and L. F. Lindoy, *J. Am. Chem. Soc.*, 1991, **113**, 3346 and unpublished work.
26 L. Fabbrizzi, *Comments Inorg. Chem.*, 1985, **4**, 33.

Received 3rd *January* 1991; *Paper* 1/00045D